Abdominal Imaging

Published online: 10 January 2014

Abdom Imaging (2014) 39:310–322
DOI: 10.1007/s00261-013-0069-6

Combined hepatocellular-cholangiocarcinoma: what the radiologist needs to know about biphenotypic liver carcinoma

Anup S. Shetty,[1] Kathryn J. Fowler,[1] Elizabeth M. Brunt,[2] Saurabh Agarwal,[1] Vamsi R. Narra,[1] Christine O. Menias[1]

[1]Mallinckrodt Institute of Radiology, Washington University School of Medicine, 510 S. Kingshighway Blvd, Campus Box 8131, Saint Louis, MO 63110, USA
[2]Department of Pathology and Immunology, Washington University School of Medicine, Saint Louis, MO 63110, USA

Abstract

Combined hepatocellular-cholangiocarcinoma (CHC), also referred to as primary liver carcinoma (PLC) with biphenotypic differentiation, is an increasingly recognized subtype of malignant PLC encompassing varying morphologic forms thought to arise either from progenitor cell lineage or dedifferentiation of mature liver cells. Tumor cells express both biliary and hepatocellular markers by immunohistochemistry, and may also express progenitor cell and stem cell markers. Due to the relative rarity of this tumor type, little is known about the risk factors, imaging appearance, or prognosis. Few studies have demonstrated risk factors that overlap with hepatocellular carcinoma (HCC) and cholangiocarcinoma (CC), though not all appear to arise in the background of cirrhosis. The imaging appearances of these tumors may overlap with those of HCC and CC and discriminating features such as classic enhancement patterns and biliary ductal dilation are not universally present. Serum tumor markers, such as alpha-fetoprotein and carbohydrate antigen 19-9, may be helpful when they are discordant with imaging or if both are elevated to a significant degree. In regards to management and prognosis, most studies demonstrate worse outcomes compared with HCC or CC. In the United States, the diagnosis of HCC is frequently made with imaging alone, and subsequent management decisions, including organ allocation for transplantation, rely upon the radiological diagnosis. Given the importance of radiological diagnosis, awareness of this tumor type is essential for appropriate management.

Correspondence to: Anup S. Shetty; *email:* shettya@mir.wustl.edu

Key words: Liver MRI—Hepatocellular carcinoma—Cholangiocarcinoma—Biphenotypic liver carcinoma—Liver transplantation

Introduction

Combined hepatocellular-cholangiocarcinoma (CHC) encompasses a spectrum of carcinomas that are primary to the liver and exhibit biphenotypic differentiation. These tumors were first described by Wells in 1903 and further characterized by Allen and Lisa in 1949 [1]. Interest has increasingly grown because of sophisticated pathologic characterization of CHC [2] and growing interest in defining the imaging features of this entity. Prospective diagnosis of CHC is of considerable interest, given the paramount role of imaging in the diagnosis of liver tumors in general and HCC in particular, the recognized overlap of clinical and imaging features between HCC and many forms of CHC, and the high stakes of this tumor in liver transplantation. This article will describe the currently understood unique pathologic features and clinical considerations of CHC, imaging features that may suggest the diagnosis, and management implications. A series of pathologically confirmed CHC cases encountered at our institution from 2006 to 2011 will illustrate the gamut of radiologic–pathologic findings.

Pathology

The most recent World Health Organization (WHO) guidelines define CHC histopathologically as a tumor with unequivocal, intermixed elements of HCC and CC [2]. Allen and Lisa's classification scheme subdivided CHC into

type A (separate foci of HCC and CC within the same liver), type B (adjacent HCC and CC comingling with continued growth), and type C (components of HCC and CC within the same mass) [1, 3]. A different scheme from Goodman et al. described type I tumors with HCC and CC within the same liver, type II tumors with transition from elements of HCC to elements of CC, and type III tumors as fibrolamellar tumors containing mucin-producing pseudoglands [1, 3]. It is now apparent that liver carcinomas with biphenotypic differentiation are even more diverse than these original descriptions, as noted in the current 2010 WHO guidelines. There are three noted subtypes with stem cell differentiation [2]; thus, for the diagnosis to be made, the tumor must have immunohistochemical (IHC) features at least of biliary (keratin 7) and hepatocellular (polyclonal carcinoembryonic antigen [pCEA] with canalicular staining) differentiation and may, in addition, show progenitor cell (keratin 19, epithelial call adhesion molecule [epCAM]) and/or stem cell (CD133, CD44) markers. Other IHC markers of interest continue to be reported in recent international symposia.

By gross evaluation, most, but not all, primary liver carcinomas (PLCs) are firm, seemingly well delineated, and lighter than the background liver. These tumors are the ones with the most stroma. The tumors that most resemble HCC lack the dense stroma, and may be more fleshy and bulge above the cut surface in a similar fashion to HCC.

The biphenotypic features of CHC are under active investigation; they are postulated to represent either evolution from liver progenitor cells or dedifferentiation of mature hepatocytes [4]. Recent studies supporting the theory of progenitor cell lineage have shown CHC tumor cells to be more primitive than HCC or CC, with positive staining for liver stem cell markers [4, 5] and downregulation of hepatocyte differentiation [5]. By light microscopy, the tumors may appear to be HCC, CC, or combinations. The stroma may be desmoplastic or not. There are several possible patterns for both the epithelial and stromal components. A number of IHC markers favoring hepatocellular differentiation have been described, include cytoplasmic hepatocyte paraffin 1 (HepPar1), thyroid transcription factor-1 (TTF-1), and a canalicular pattern of staining with pCEA (Fig. 1) and/or CD-10 [6–9]. It is important to note that not all of these IHC markers are consistently positive, and, as noted above, the canalicular markers are the most reliable proof. Biliary differentiation is noted by keratin 7 (K7) and keratin 19 (K19) reactivities [4, 9, 10]. Expression of K7 or K19 in HCC has been shown to correlate with more aggressive disease and rapid recurrence [10]. These tumors are commonly present within a desmoplastic stroma, not unlike that of cholangiocarcinoma (CC). At our institution, CHC is considered when a liver carcinoma has appropriate morphologic characteristics and IHC analysis positive for tumor cells with K7 or K19 and a canalicular pattern of reactivity with pCEA or CD10.

Clinical considerations

CHC is said to account for 0.4–14% of PLCs in the literature [1, 11–13], although these tumors likely have not been fully appreciated in the past, as many have either been diagnosed as CC or hepatocellular carcinoma. Given the relative rarity of studies of CHC, patient demographic and clinical data have been extrapolated from small case series, highlighting geographic variations in incidence and risk factors between Asian and western populations [3]. Asian case series have demonstrated CHC more frequently in an older male population with chronic hepatitis and cirrhosis, frequently from hepatitis B [4, 12, 13]. A few US series demonstrate a more balanced gender distribution and patients frequently without chronic liver disease [1, 14], matching our own institutional experience.

Risk factors are reported to include those of HCC, including any cause of cirrhosis (e.g., alcohol misuse, viral hepatitis, etc.) and CC (primary sclerosing cholangitis) [3, 13]. However, cases also occur in noncirrhotic patients, and underlying risk factors are unknown. As with HCC and CC, insidious onset of CHC with late presentation of advanced disease has been reported [3]. Symptoms include abdominal pain, jaundice, swelling referable to ascites, fatigue, weight loss, pruritus, fever, hepatomegaly, and cholangitis.

Serum tumor markers of potential utility in CHC are CA 19-9 and AFP, which are associated with CC and HCC, respectively [3]. While neither marker alone is sensitive or specific for CHC, when both are simultaneously elevated or elevated in discordance with presumptive imaging findings (i.e., elevated CA 19-9 with imaging findings of HCC, or elevated AFP with imaging findings of CC), CHC should at least be considered [4, 14, 15].

Review of imaging modalities and protocols

Dynamic contrast-enhanced magnetic resonance imaging (MRI) and computed tomography (CT) are the imaging modalities of choice in the evaluation of CHC, especially MRI, given its absence of ionizing radiation and superior contrast resolution [16]. In a small series comparing sensitivity of detection of CHC, MRI was 100% sensitive, compared with 78% for CT [17].

MR examinations may be performed with a 1.5 T or 3.0 T system using an abdominal-phased array coil. A liver MRI examination should consist of multiplanar single-shot fast spin echo T2-weighted, fat-suppressed T2-weighted, dual echo chemical shift T1-weighted, pre- and dynamic postcontrastfast-suppressed T1-weighted, and diffusion-weighted images, along with magnetic

Table 1. Summary of imaging findings

Patient	CA19-9	AFP	Arterial enhancement	Delayed enhancement	Washout	Capsular retraction	Biliary ductal dilatation	Other features
59-year-old woman	Normal	N/A	Peripheral	–	+	–	–	–
60-year-old woman with cirrhosis	Normal	Normal	Diffuse	–	+	+	–	Diffusion restriction
58-year-old woman	Elevated	Normal	Peripheral	+	–	+	–	–
49-year-old man with hepatitis B	Elevated	Normal	Peripheral	–	+	–	+	Tumor thrombus
72-year-old woman with hereditary hemochromatosis	N/A	Normal	Peripheral	–	–	–	–	–
77-year-old man	N/A	N/A	–	+	+	+	–	–
89-year-old woman	Normal	Elevated	Peripheral	+	–	+	–	Diffusion restriction
62-year-old man with hepatitis C	Elevated	Elevated	Peripheral	–	–	–	–	–

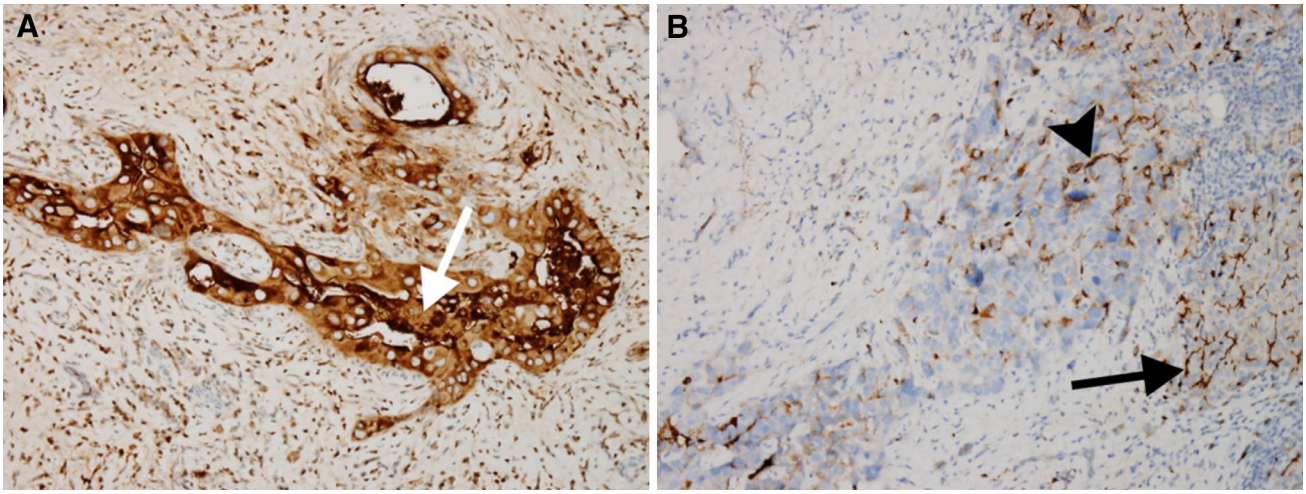

Fig. 1. Immunohistochemical liver stains with polyclonal carcinoembryonic antigen (pCEA) in a patient with CHC. **A** Diffuse cytoplasmic pattern of staining in this abortive gland-like structure highlights the nearly pure CC component (*white arrow*). **B** Hepatocellular differentiation of the tumor in the same patient is demonstrated by canalicular pattern of reactivity and lack of cytoplasmic reactivity. (*black arrowhead*). In nontumor tissue parenchyma, canalicular reactivity is found only in hepatic tissue (*black arrow*).

resonance cholangiopancreatography (MRCP) sequences to evaluate for ductal involvement. Hepatobiliary phase imaging may also be performed with gadobenate dimeglumine (Multihance, Bracco Diagnostics, Milan, Italy) with a 60-min delay or gadoxetate disodium (Eovist, Bayer Healthcare, Wayne, NJ) with a 20-min delay.

Our CT liver protocol consists of multiphase dynamic imaging with thin-collimation noncontrast, arterial, portal venous, and delayed phase images.

Imaging features

Few studies have been published describing the radiologic characteristics of CHC [14, 18–20]. The well-known imaging features of HCC and CC provide a framework from which to approach CHC. Characteristic findings of HCC on CT and MRI include arterial enhancement with washout on portal venous or equilibrium phase imaging, and an enhancing pseudocapsule on delayed images [16]. An additional feature more clearly identified on MRI is intratumoral lipid, and scirrhous HCC may demonstrate a more fibrotic pattern of progressive enhancement. Characteristic findings of CC on CT and MRI include peripheral arterial rim enhancement with progressive centripetal enhancement of fibrous stroma, capsular retraction, and associated biliary ductal dilatation. A T2 hypointense scar may be seen on MRI. Nonspecific features of each tumor evident on MRI include T1 hypointensity, T2 hyperintensity, diffusion restriction, vascular invasion, and tumor thrombus, with hypermetabolic activity identified on PET imaging. Lymph node metastases are more common with CC than HCC [20]. The presence of imaging features of both HCC and CC in the same tumor should alert the radiologist to the possibility of CHC.

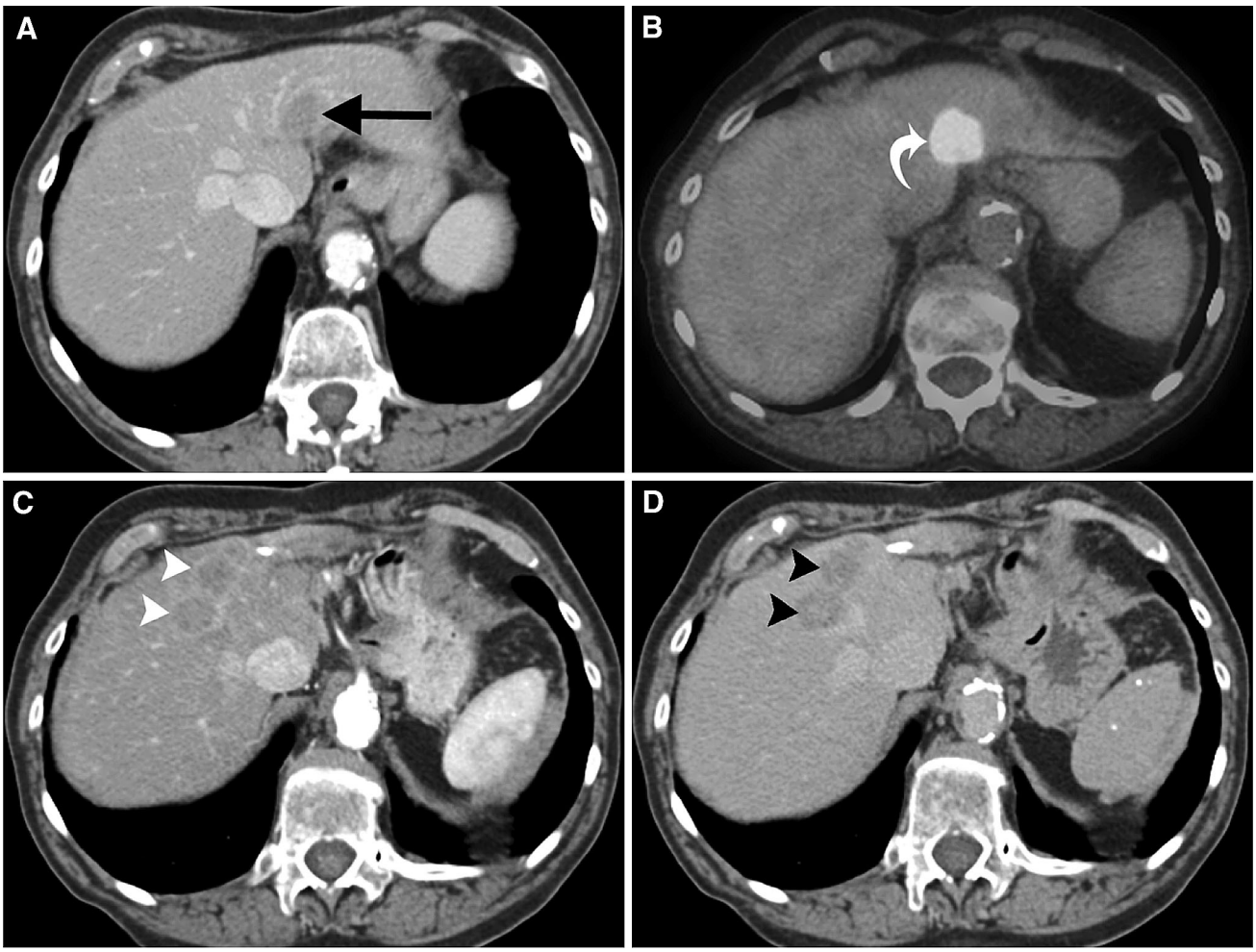

Fig. 2. CHC in an 83-year-old noncirrhotic woman. **A**, **B** Axial-enhanced CT and fused PET/CT demonstrate a rim-enhancing, centrally hypoattenuating (*black arrow*), hypermetabolic mass (*curved white arrow*) in the left hemiliver. **C**, **D** After completing chemotherapy, axial arterial-enhanced and 4-min-delayed CT demonstrates multiple peripherally arterial enhancing masses (*white arrowheads*) with delayed washout (*black arrowheads*).

Although imaging features of both HCC and CC are often present in CHC, many of the CHC tumors encountered at our institution more closely resemble CC (Table 1). The following cases demonstrate the varied appearances of CHC.

Case 1 presents an 83-year-old woman with normal CA 19-9 (no AFP level was obtained). Initial imaging demonstrated a mass with imaging features more characteristic of CC (Fig. 2). Core liver biopsy performed at an outside facility was reviewed by our pathologists, and demonstrated tumor cells positive for K7, with morphology and immunohistochemistry favoring a primary CC over metastatic adenocarcinoma from a biliary, upper gastrointestinal tract, or pulmonary origin. The patient was treated with surgical resection of hepatic segment 2. Tumor cells were positive for K7 and K19, and positive for canalicular reactivity of pCEA, consistent with a PLC with biphenotypic differentiation. Six-month follow-up imaging demonstrated multiple new liver lesions with imaging features more characteristic of HCC (Fig. 2) and metastatic disease to the omentum, bone, and retroperitoneal lymph nodes. She was subsequently treated with gemcitabine for two cycles, and ultimately opted for hospice care.

Case 2 presents a cirrhotic 60-year-old woman with normal AFP and CA 19-9. She initially presented with right upper quadrant abdominal pain. The imaging features in this case combine characteristic elements of HCC and CC (Fig. 3). Fine needle aspiration via endoscopic ultrasound of a lesion in the left hemiliver demonstrated biphenotypic PLC with tumor cells positive for focal canalicular reactivity of CD10 and pCEA, and strongly positive for K19. The patient was treated initially with transarterial chemoembolization of the right hemiliver with doxorubicin and Lipiodol, with response in the treated tumor but progressive disease elsewhere in the liver. Subsequent therapy with gemcitabine and oxaliplatin was halted after continued disease progression was

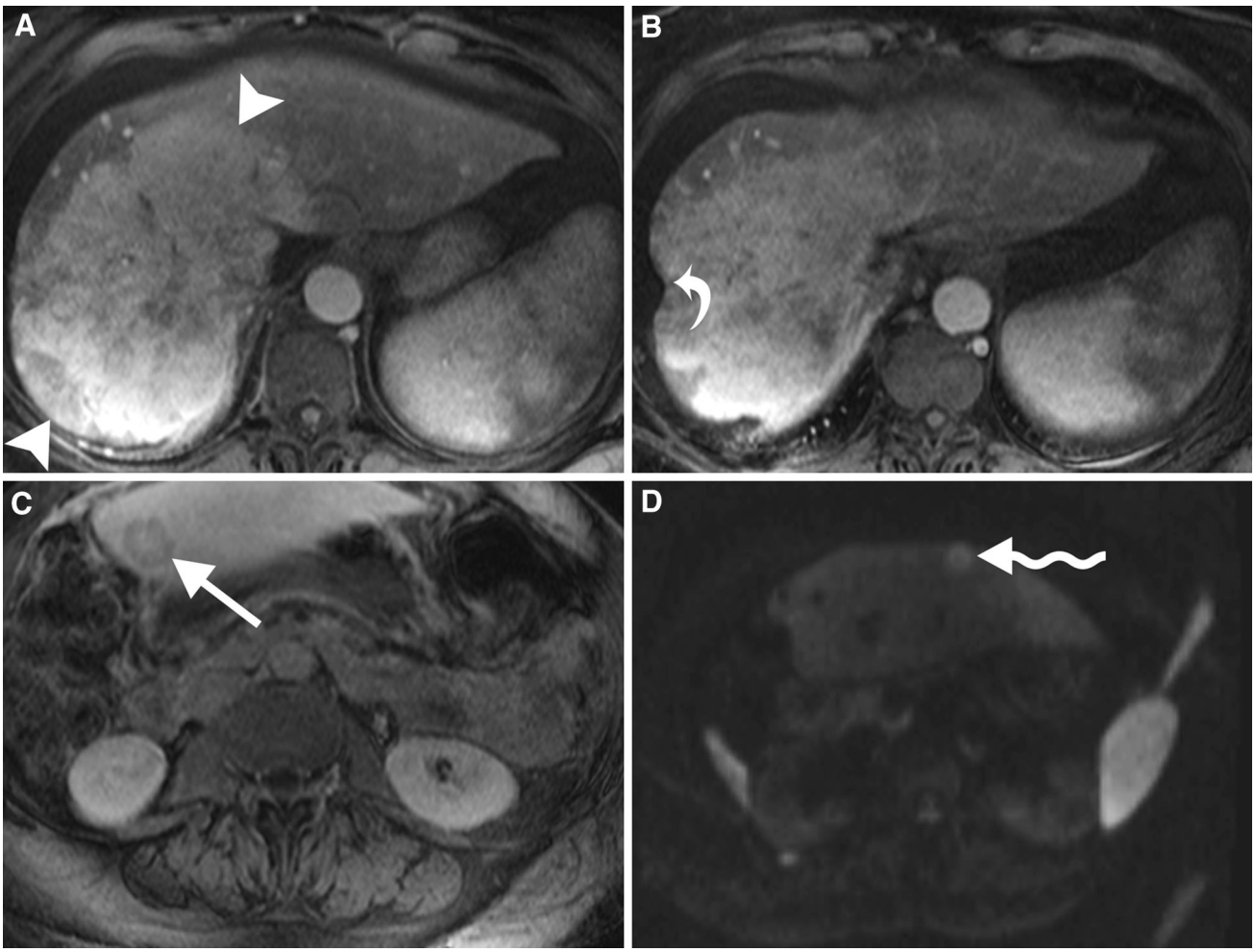

Fig. 3. CHC in a 60-year-old cirrhotic woman with mixed imaging features. **A**, **B** Axial T1 VIBE arterially enhanced MRI demonstrates a dominant arterially enhancing mass extending from the right hemiliver into the left (*white arrowheads*) with capsular retraction (*curved white arrow*). **C** Axial T1 VIBE 5-min-delayed enhanced MRI demonstrates washout of an intrahepatic metastasis in the left hemiliver (*white arrow*). **D** Axial diffusion-weighted MRI demonstrates diffusion restriction of an additional intrahepatic metastasis in the left hemiliver (*white squiggly arrow*).

demonstrated on MRI. Selective internal radiotherapy of the dominant right hemiliver lesion, and multicentric disease in the left hemiliver was then performed sequentially with yttrium-90 radioembolization. Her liver disease remained stable thereafter for 6 months, although she developed peritoneal carcinomatosis, diaphragmatic invasion from a liver lesion, and osseous metastatic disease.

Case 3 presents a noncirrhotic 58-year-old woman with normal AFP and elevated CA 19-9 (983.5 units/mL). She initially presented with right upper quadrant and epigastric abdominal pain. As in case 1, the features of images are more characteristic of CC (Fig. 4). Ultrasound-guided core biopsy demonstrated PLC with biphenotypic differentiation, with tumor cells staining positive for K7 and K19 and demonstrating canalicular reactivity for pCEA and CD10. The patient received neoadjuvant chemotherapy with gemcitabine and cisplatin, followed by liver trisegmentectomy again demonstrating CHC (CC predominant), with lymphatic and vascular invasion. The complex surgery required venovenous bypass with cold preservation and biliary reconstruction with roux-en-Y hepaticojejunostomy, which ultimately was complicated by anastomotic leak necessitating an exploratory laparotomy for revision of the hepaticojejunostomy two days after the initial surgery. She remained hospitalized for the next three weeks and ultimately expired because of gastrointestinal bleeding.

Case 4 presents a 49-year-old man with hepatitis B, normal AFP and slightly elevated CA 19-9 (39.8 units/mL). He presented with abdominal pain, was diagnosed with portal vein thrombosis and was treated with anticoagulation. Four months later, he developed jaundice followed by hematemesis related to esophageal varices. The imaging demonstrates the gamut of imaging features of CHC (Fig. 5). Percutaneous core biopsy demonstrated

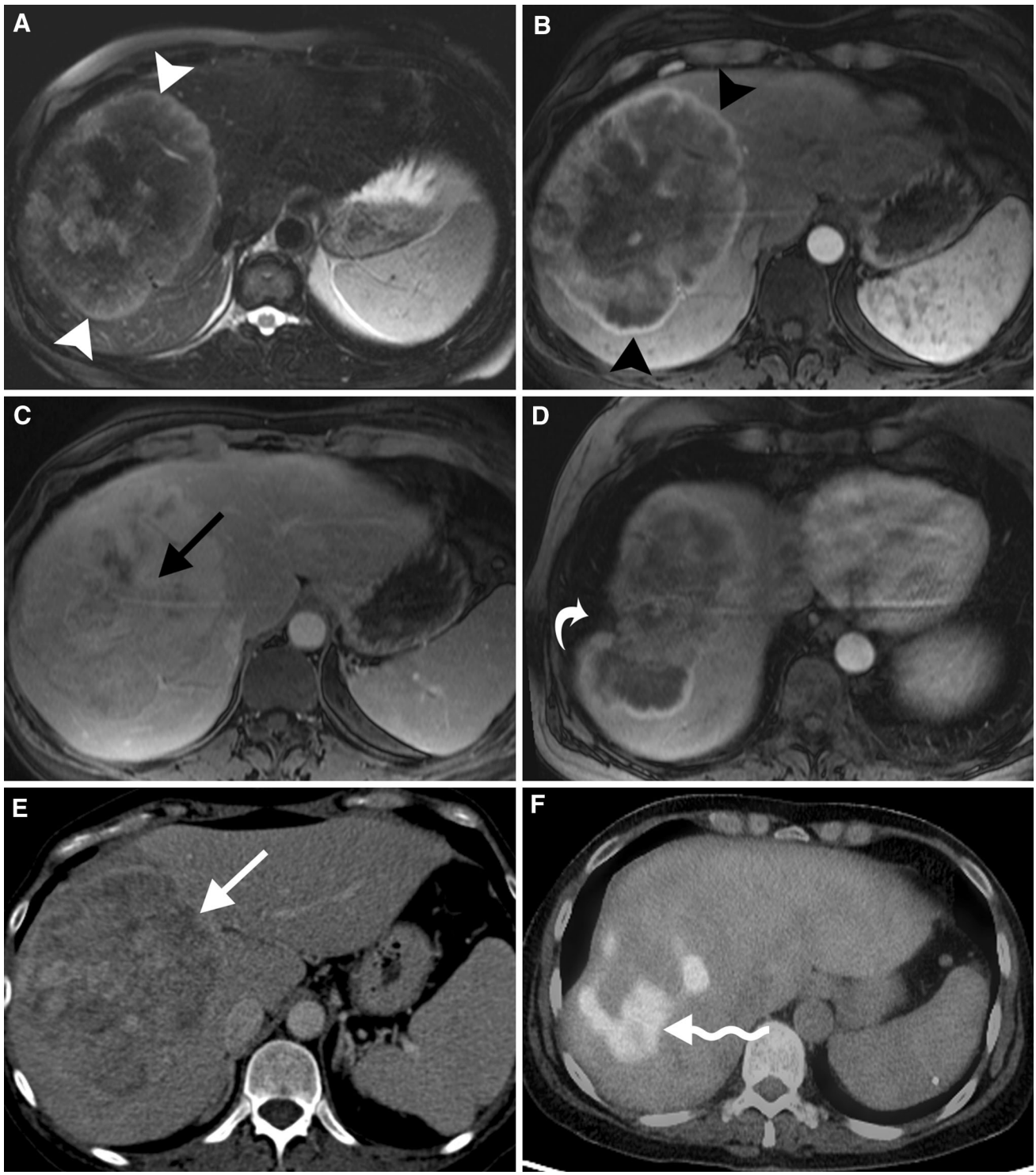

Fig. 4. CHC in a 58-year-old noncirrhotic woman with imaging features more typical of CC. **A** Axial T2 inversion-recovery MRI demonstrates a heterogeneously T2 hyperintense mass in the right hemiliver (*white arrowheads*). **B**–**D** Axial T1 VIBE contrast-enhanced arterial and 5-min-delayed MRI demonstrates peripheral arterial enhancement (*black arrowheads*) with progressive centripetal enhancement (*black arrow*) and capsular retraction (*curved white arrow*). **E**, **F** Axial-enhanced CT and fused PET/CT demonstrate a peripherally enhancing mass (*white straight arrow*) with peripherally hypermetabolic activity (*white squiggly arrow*).

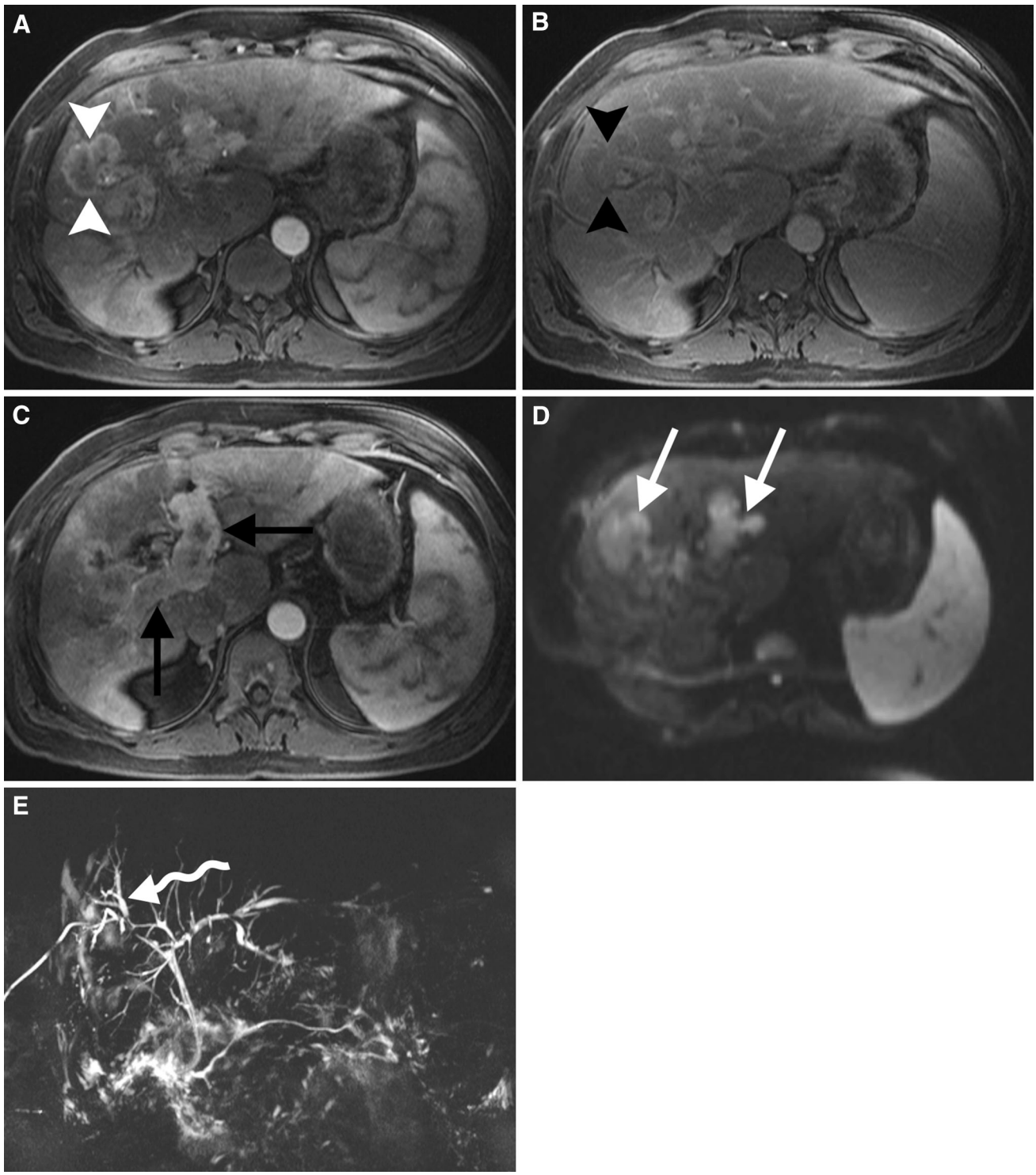

Fig. 5. CHC in a 49-year-old man with chronic hepatitis B, with mixed imaging features. **A**, **B** Axial T1 VIBE contrast-enhanced arterial and 5-min-delayed MRI demonstrates a peripherally enhancing mass (*white arrowheads*) with delayed washout (*black arrowheads*). **C** Axial T1 VIBE contrast-enhanced arterial phase MRI demonstrates enhancing tumor thrombus filling the right and left portal veins (*black arrows*). **D** Axial diffusion-weighted MRI demonstrates diffusion restriction of the mass and tumor thrombus (*white arrows*). **E** Coronal thick-slab MRCP demonstrates mild biliary ductal dilatation in the right hemiliver associated with the mass (*white squiggly arrow*).

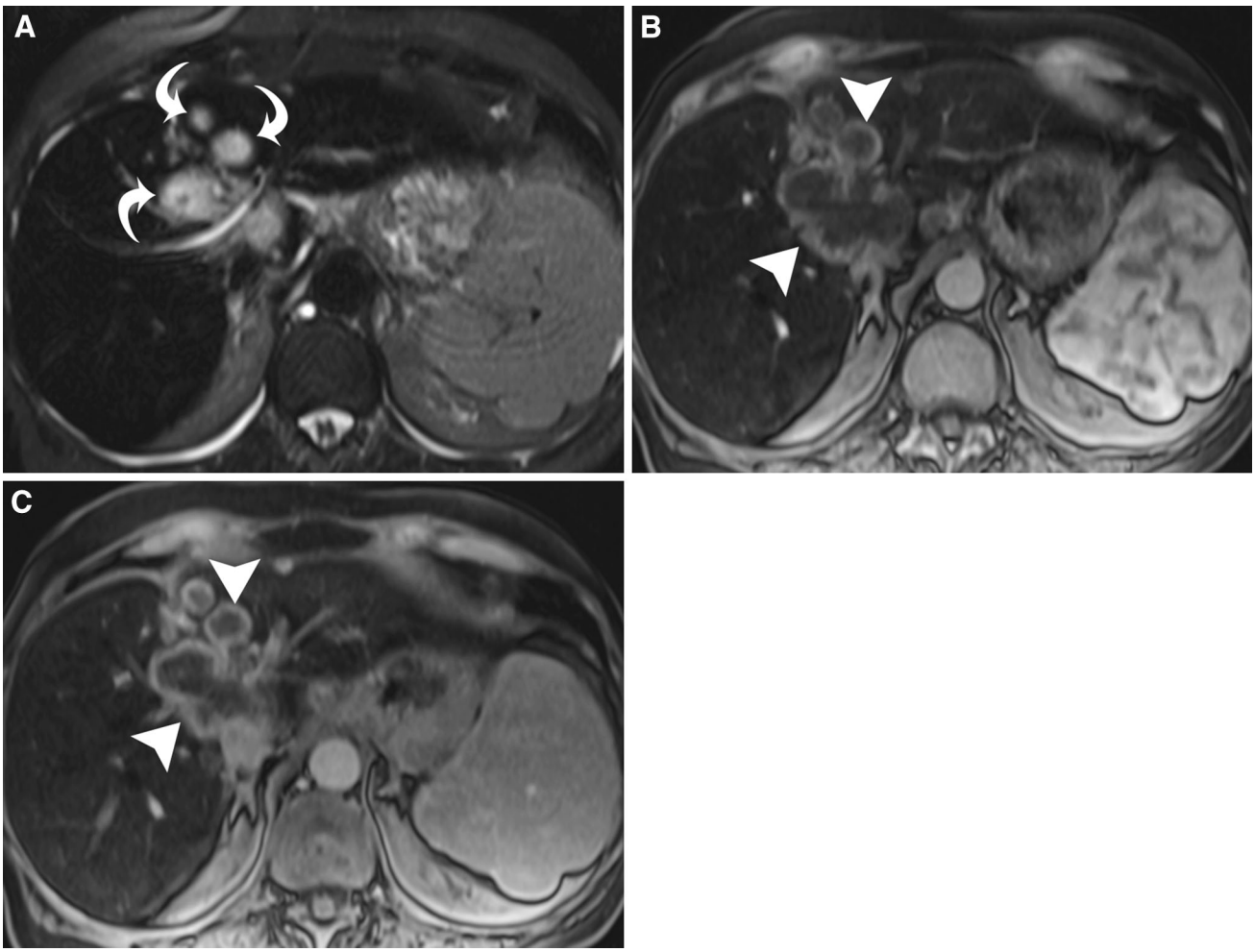

Fig. 6. CHC in a 72-year-old noncirrhotic woman with hereditary hemochromatosis and more typical imaging features of CC. **A** Axial T2 fat-saturated MRI demonstrates multiple T2 hyperintense masses (*curved white arrows*) in a background of diffusely T2 hypointense liver parenchyma, in keeping with the patient's underlying hemochromatosis. **B**, **C** Axial T1 VIBE contrast-enhanced arterial phase and 5-min-delayed MRI demonstrate peripheral arterial enhancement of the masses without delayed washout (*white arrowheads*).

biphenotypic PLC, positive for K7 and K19, and canalicular reactivity of pCEA. The patient subsequently returned to his referring physician for further treatment.

Case 5 presents a 72-year-old noncirrhotic woman with myelodysplastic syndrome, hereditary hemochromatosis and normal AFP. She presented with flank pain and recurrent urinary tract infections, at which time a large liver mass was incidentally found on renal sonography. The imaging features are again more typical of CC (Fig. 6). Ultrasound-guided core liver biopsy demonstrating PLC with mixed biliary and hepatocellular differentiation, with strong and diffuse K19 positivity, focal positively for K7, and canalicular reactivity of pCEA and CD10. Treatment with half-dose sorafenib was poorly tolerated and the patient succumbed to her disease within the next month.

Case 6 presents a 77-year-old noncirrhotic man initially evaluated for a right upper lobe mass and incidentally found to have a mass in the right hemiliver (AFP and CA 19-9 were not measured). The imaging features are more consistent with CC (Fig. 7). Ultrasound-guided core liver biopsy demonstrated PLC with biphenotypic features. K7 and K19 were strongly positive in all tumor cells. A canalicular reactivity pattern of pCEA was demonstrated, with no CD10 reactivity. Squamous cell carcinoma was subsequently demonstrated upon biopsy of the right upper lobe mass. The patient was treated with definitive stereotactic radiotherapy for the lung mass and underwent laparoscopic partial hepatectomy. IHC of the resected tumor confirmed the previous biopsy findings. The patient was subsequently lost to follow-up.

Case 7 presents an 89-year-old noncirrhotic woman with elevated AFP (25 ng/mL) and normal CA 19-9. She presented with peripheral neuropathy and underwent CT of the chest, abdomen, and pelvis as part of an evaluation for paraneoplastic syndrome, with subsequent PET/CT and MRI. Imaging features are more characteristic of

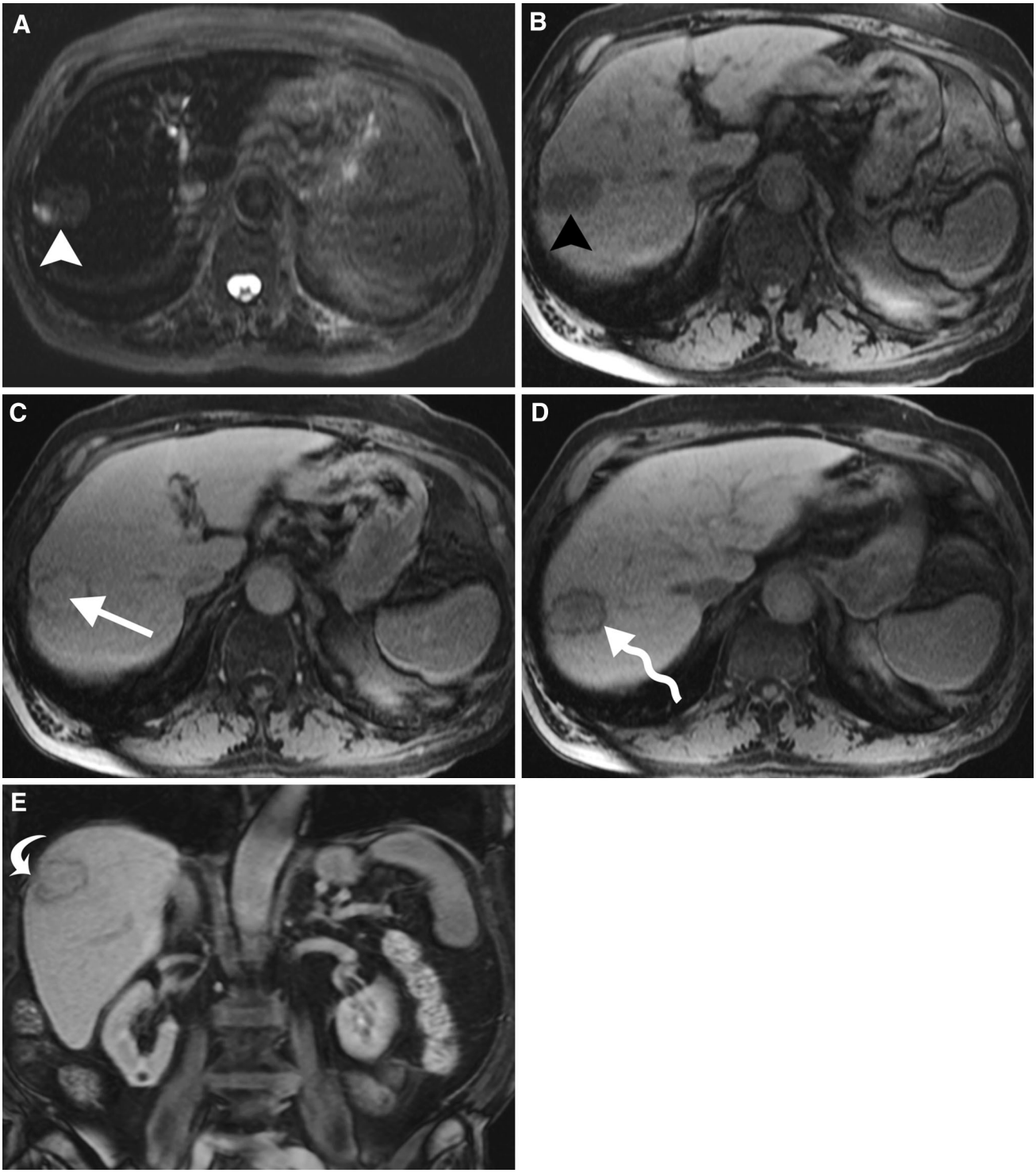

Fig. 7. CHC in a 77-year-old noncirrhotic man with imaging features more characteristic of CC. **A** Axial T2 fat-suppressed MRI demonstrates a T2 hyperintense mass (*white arrowhead*) at the junction of segments 7/8. **B–D** Axial T1 VIBE precontrast and dynamic-enhanced MRI demonstrate T1 hypointensity (*black arrowhead*), progressive central enhancement (*white arrow*), and delayed peripheral washout (*squiggly white arrow*). **E** Coronal T1 VIBE postcontrast MRI demonstrates capsular retraction (*curved white arrow*).

CC (Fig. 8). Ultrasound-guided core liver biopsy demonstrated PLC with biphenotypic differentiation. Tumor cells were positive for K7. Canalicular reactivities with pCEA and CD10 were present. The patient was initially treated with transarterial chemoembolization with Doxorubicin, Lipiodol and gelfoam, with approximately

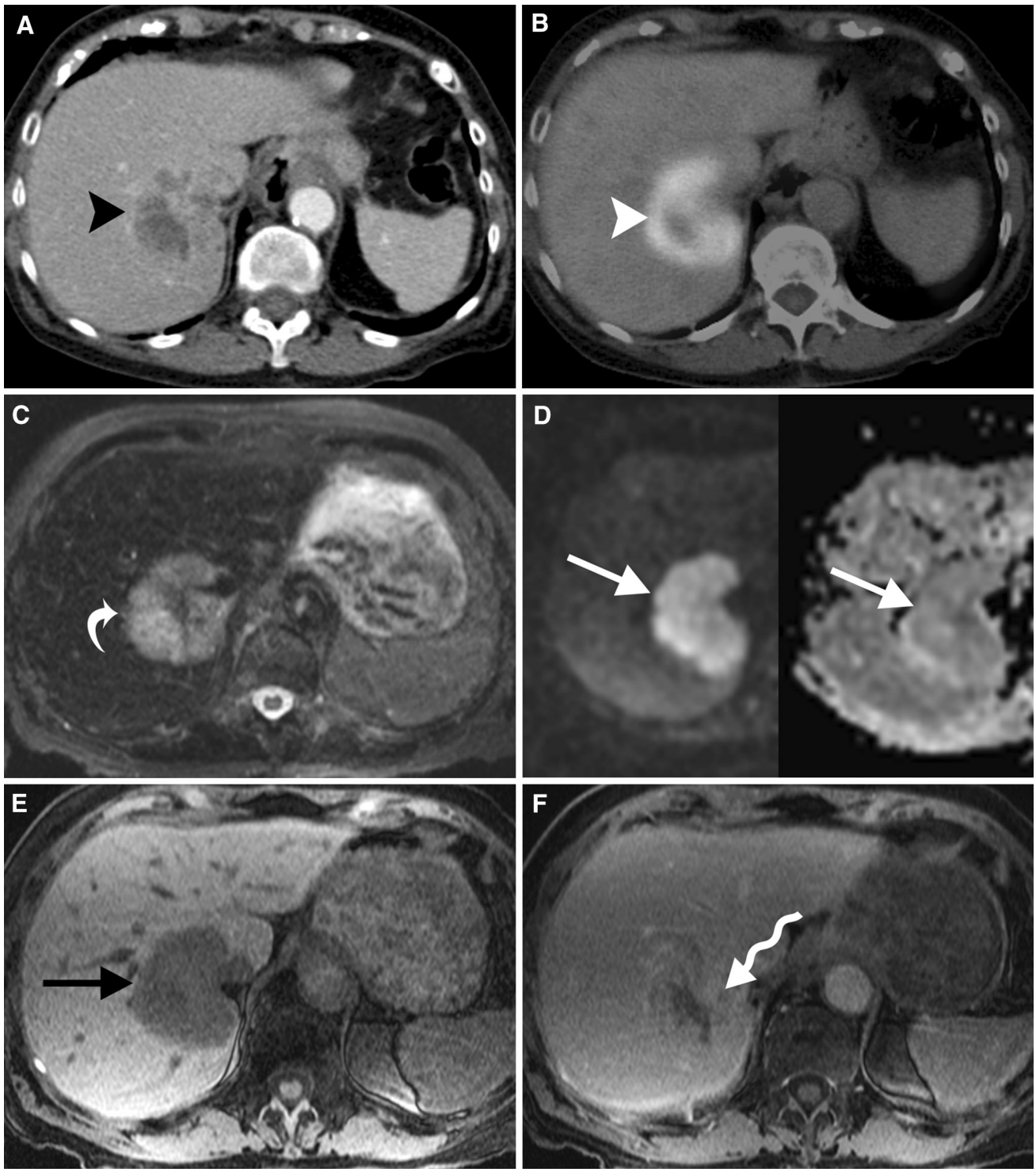

Fig. 8. CHC in an 89-year-old noncirrhotic woman with imaging features of CC. **A** Axial-enhanced CT demonstrates a peripherally enhancing, centrally hypoattenuating large right hemiliver mass (*black arrowhead*). **B** Axial-fused PET/CT demonstrates avid FDG-uptake within the mass (*white arrowhead*). **C** Axial T2 fat-suppressed MRI demonstrates T2 hyperintensity of the mass (*curved white arrow*). **D** Axial DWI (b = 800) and ADC demonstrate marked diffusion restriction of the mass (*white arrows*). **E**, **F** Axial T1 VIBE precontrast and delayed MRI demonstrate T1 hypointensity (*black arrow*) and progressive central enhancement of the mass (*squiggly white arrows*).

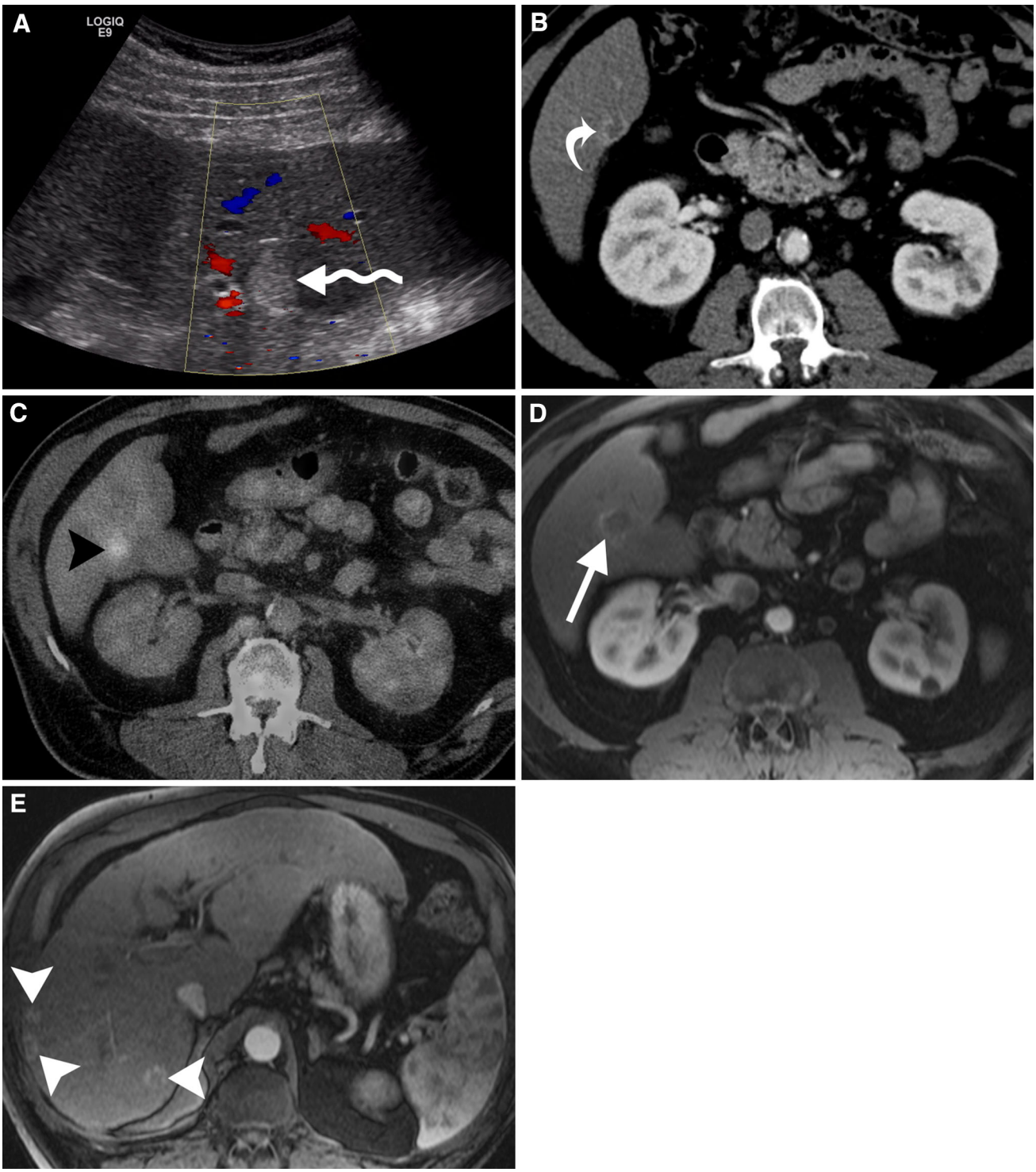

Fig. 9. CHC in a 62-year-old man with hepatitis C and cirrhosis, with mixed imaging features. **A** Ultrasound demonstrates a hyperechoic liver mass without internal Doppler flow (*squiggly white arrow*). **B** Axial arterial-phase-enhanced CT demonstrates a peripherally enhancing segment 6 lesion (*curved white arrow*). **C** Axial-fused PET-CT demonstrates abnormal increased FDG uptake within the mass (*black arrowhead*). **D** Axial T1 VIBE arterial-phase-enhanced MRI demonstrates peripheral arterial enhancement (*white arrow*). **E** Subsequent axial T1 VIBE arterially enhanced MRI demonstrates multiple new peripherally enhancing masses, likely intrahepatic metastases (*white arrowheads*).

60% tumor response. Right portal vein embolization was performed to induce hypertrophy of the future liver remnant in anticipation of resection. Preoperative imaging demonstrated growth of the mass, and the patient ultimately underwent extended right hepatectomy with vena caval reconstruction. IHC of the resected tumor was positive for K7 and K19, with canalicular reactivity of pCEA, confirming a PLC with biphenotypic differentiation. Her postoperative course was complicated by hepatic infarction and multisystem organ failure, and the patient expired in the intensive care unit 5 days after surgery.

Case 8 presents a 62-year-old man with chronic hepatitis C, cirrhosis, and mildly elevated AFP (20 ng/mL) and CA 19-9 (37 units/mL). He presented with a hyperechoic mass on routine screening liver sonography for HCC. Mixed imaging features of HCC and CC are seen (Fig. 9). Ultrasound-guided core liver biopsy demonstrated PLC with areas of varying differentiations of CC and HCC. Within foci of morphologically suggested CC, K19 was positive. CD10 reactivity was variably membranous and canalicular in different areas of the tumor, as was pCEA. The patient underwent transarterial chemoembolization of the right hemiliver with cisplatin, doxorubicin, mitomycin, and gelfoam, followed by an additional treatment two months later with doxorubicin, Lipiodol, and gelfoam, without tumor response. Percutaneous cryoablation of the tumor was next attempted, with evidence of disease progression on subsequent MRI, manifested by development of multiple ring-enhancing intrahepatic metastases and periportal lymphadenopathy (Fig. 9). Treatment with sorafenib initially resulted in a response with decrease in lymphadenopathy and resolution of enhancement of the intrahepatic metastases, with subsequent growth of lymphadenopathy. Two years after initial diagnosis, the patient was still alive and being treated with sorafenib.

Management

The prognosis of CHC compared with HCC or CC remains uncertain because of the relative unknown nature and difficulty defining these tumors. A majority of studies have demonstrated worse overall survival of CHC, with a minority showing an intermediate prognosis between HCC and CC [1, 11, 13, 17, 21–23]. Treatment options include liver transplantation, resection, transarterial chemoembolization (TACE), local ablative therapy such as radiofrequency ablation, and chemotherapy [13, 22, 24, 25]. While an optimal treatment algorithm has yet to be defined, radical resection offers patients the longest overall survival (16.5 months) versus nonoperative treatment modalities [13]. Tumor recurrence is frequent after resection, with a median time to recurrence of 6–9 months [13, 23]. Recurrent tumors often are hypovascular and fibrotic, potentially limiting the utility of TACE and raising consideration for local ablative therapy under this circumstance [1, 22]. Experience with chemotherapy in treatment of patients with CHC is limited, with a case report detailing survival prolongation in a patient with CHC and distant metastatic disease [25]. A current investigational approach into treatment for patients with unresectable CC combines chemotherapy with gemcitabine and platinum-based therapy [26] with hepatic artery infusion pump therapy with floxuridine [27].

Several series of patients with CHC discovered after liver transplantation for presumed HCC highlight the importance of considering the diagnosis of CHC before transplantation. Liver transplant is accepted as an effective curative treatment for selected patients with HCC, with a 5-year survival rate exceeding 70% [24, 28]. However, CC is generally considered a contraindication for liver transplantation because of the risk of tumor recurrence [24]. In a series of patients transplanted for presumptive HCC, pathologic analysis of the explanted liver demonstrated a 3% rate of CHC or CC rather than HCC in these patients [24]. The 5-year recurrence rate of CHC in these patients was 78%, compared with only 17% in patients with HCC. These patients demonstrated shorter disease-free survival and a higher recurrence rate than transplanted patients with retrospectively discovered CC.

Conclusion

Approximately 20% of liver transplants in the US are performed for HCC [24]. Current guidelines for transplantation do not require pathologic proof of HCC if the imaging features on dynamic contrast-enhanced MRI or CT are concordant [28]. CHC is currently thought to be a relatively rare subtype of PLC and shares imaging features of HCC and CC, with prognosis closer to that of CC than HCC. Accurate prospective diagnosis, although difficult, can be suggested when imaging features and tumor markers either overlap HCC and CC or are discordant. In these patients, biopsy and careful pathologic analysis should be performed to guide appropriate therapy and avoid liver transplantation given the high risk of recurrence in patients with CHC.

Reference

1. Jarnagin WR, Weber S, Tickoo SK, et al. (2002) Combined hepatocellular and cholangiocarcinoma: demographic, clinical, and prognostic factors. Cancer 94(7):6–2040
2. Theise ND, Nakashima O, Park YN, Nakanuma Y (2010) Combined hepatocellular-cholangiocarcinoma. In: Bosman FT, Carneiro F, Hruban RH, Theise ND (eds) *Who classification of tumours of the digestive system*, 4th edn. Lyon: International Agency for Research on Cancer, pp 225–227
3. Kassahun WT, Hauss J (2008) Management of combined hepatocellular and cholangiocarcinoma. Int J Clin Pract 62(8):8–1271
4. Yu XH, Xu LB, Zeng H, et al. (2011) Clinicopathologic analysis of 14 patients with combined hepatocellular carcinoma and cholangiocarcinoma. Hepatobiliary Pancreat Dis Int 10(6):5–620

5. Coulouarn C, Cavard C, Rubbia-Brandt L, et al. (2012) Combined hepatocellular-cholangiocarcinomas exhibit progenitor features and activation of Wnt and TGFβ signaling pathways. Carcinogenesis 33(9):6–1791
6. Itoyama M, Hata M, Yamanegi K, et al. (2012) Expression of both hepatocellular carcinoma and cholangiocarcinoma phenotypes in hepatocellular carcinoma and cholangiocarcinoma components in combined hepatocellular and cholangiocarcinoma. Med Mol Morphol 45(1):7–13
7. Al-Muhannadi N, Ansari N, Brahmi U, Satir AA (2011) Differential diagnosis of malignant epithelial tumours of the liver: an immunohistochemical study on liver biopsy. Ann Hepatol 10(4):508–515
8. Lei JY, Bourne PA, DiSant'Agnese PA, Huang J (2006) Cytoplasmic staining of TTF-1 in the differential diagnosis of hepatocellular carcinoma vs cholangiocarcinoma and metastatic carcinoma of the liver. Am J Clin Pathol 125(4):25–519
9. Lefkowitch JH (ed) (2010) Neoplasms and nodules. In: *Scheuer's liver biopsy interpretation*, 8th edn. London: Saunders Elsevier, pp 181–232
10. Zhang F, Chen XP, Zhang W, et al. (2008) Combined hepatocellular cholangiocarcinoma originating from hepatic progenitor cells: immunohistochemical and double-fluorescence immunostaining evidence. Histopathology 52(2):32–224
11. Wang J, Wang F, Kessinger A (2010) Outcome of combined hepatocellular and cholangiocarcinoma of the liver. J Oncol. http://www.ncbi.nlm.nih.gov/pmc/articles/PMC2939443/. Accessed 1 Feb 2013
12. Lee CH, Hsieh SY, Chang CJ, Lin YJ (2013) Comparison of clinical characteristics of combined hepatocellular-cholangiocarcinoma and other primary liver cancers. J Gastroenterol Hepatol 28(1):7–122
13. Yin X, Zhang BH, Qiu SJ, et al. (2012) Combined hepatocellular carcinoma and cholangiocarcinoma: clinical features, treatment modalities, and prognosis. Ann Surg Oncol 19(9):76–2869
14. de Campos RO, Semelka RC, Azevedo RM, et al. (2012) Combined hepatocellular carcinoma-cholangiocarcinoma: report of MR appearance in eleven patients. J Magn Reson Imaging 36(5):47–1139
15. Tang D, Nagano H, Nakamura M, et al. (2006) Clinical and pathological features of Allen's type C classification of resected combined hepatocellular carcinoma and cholangiocarcinoma: a comparative study with hepatocellular carcinoma and cholangiocellular carcinoma. J Gastrointest Surg 10(7):98–987
16. Fowler KJ, Brown JJ, Narra VR (2011) Magnetic resonance imaging of focal liver lesions: approach to imaging diagnosis. Hepatology 54(6):37–2227
17. Panjala C, Senecal DL, Bridges MD, et al. (2010) The diagnostic conundrum and liver transplantation outcome for combined hepatocellular-cholangiocarcinoma. Am J Transplant 10(5):7–1263
18. Hwang J, Kim YK, Park MJ, et al. (2012) Differentiating combined hepatocellular and cholangiocarcinoma from mass-forming intrahepatic cholangiocarcinoma using gadoxetic acid-enhanced MRI. J Magn Reson Imaging 36(4):9–881
19. Ebied O, Federle MP, Blachar A, et al. (2003) Hepatocellular-cholangiocarcinoma: helical computed tomography findings in 30 patients. J Comput Assist Tomogr 27(2):24–117
20. Nishie A, Yoshimitsu K, Asayama Y, et al. (2005) Detection of combined hepatocellular and cholangiocarcinomas on enhanced CT: comparison with histologic findings. AJR Am J Roentgenol 184(4):62–1157
21. Koh KC, Lee H, Choi MS, et al. (2005) Clinicopathologic features and prognosis of combined hepatocellular cholangiocarcinoma. Am J Surg 189(1):5–120
22. Liu CL, Fan ST, Lo CM, et al. (2003) Hepatic resection for combined hepatocellular and cholangiocarcinoma. Arch Surg 138(1):86–90
23. Lee JH, Chung GE, Yu SJ, et al. (2011) Long-term prognosis of combined hepatocellular and cholangiocarcinoma after curative resection comparison: comparison with hepatocellular carcinoma and cholangiocarcinoma. J Clin Gastroenterol 45(10):69–75
24. Sapisochin G, Fidelman N, Roberts JP, Yao FY (2011) Mixed hepatocellular cholangiocarcinoma and intrahepatic cholangiocarcinomain patients undergoing transplantation for hepatocellular carcinoma. Liver Transpl 17(8):42–934
25. Chi M, Mikhitarian K, Shi C, Goff LW (2012) Management of combined hepatocellular-cholangiocarcinoma. Gastrointest Cancer Res 5(6):199–202
26. Valle J, Wasan H, Palmer DH, et al. (2010) Cisplatin plus gemcitabine for biliary tract cancer. N Eng J Med 362(14):81–1273
27. Chapman W, Tan BR, Doyle M, et al. Pilot study of hepatic arterial infusion in treating patients with locally advanced, non-metastatic cholangiocarcinoma. http://clinicaltrials.gov/ct2/show/record/NCT01525069. Accessed 16 Feb 2013
28. Purysko AS, Remer EM, Coppa CP, et al. (2012) LI-RADS: a case-based review of the new categorization of liver findings in patients with end-stage liver disease. Radiographics 32(5):95–1977